

Interaction-Enhanced Group Velocity of Bosons in the Flat Band of an Optical Kagome Lattice

Tsz-Him Leung^{ⓧ,1}, Malte N. Schwarz^{ⓧ,1,2}, Shao-Wen Chang^{ⓧ,1}, Charles D. Brown^{ⓧ,1},
Govind Unnikrishnan,³ and Dan Stamper-Kurn^{1,4}

¹*Department of Physics, University of California, Berkeley, California 94720, USA*

²*Fakultät für Physik und Astronomie, Universität Würzburg, 97074 Würzburg, Germany*

³*Institut für Experimentalphysik und Zentrum für Quantenphysik, Universität Innsbruck, 6020 Innsbruck, Austria*

⁴*Materials Sciences Division, Lawrence Berkeley National Laboratory, Berkeley, California 94720, USA*



(Received 15 July 2020; revised 28 August 2020; accepted 9 September 2020; published 21 September 2020; corrected 29 September 2020)

Geometric frustration of particle motion in a kagome lattice causes the single-particle band structure to have a flat s -orbital band. We probe this band structure by placing a Bose-Einstein condensate into excited Bloch states of an optical kagome lattice, and then measuring the group velocity through the atomic momentum distribution. We find that interactions renormalize the band structure, greatly increasing the dispersion of the third band, which is nearly non-dispersing in the single-particle treatment. Calculations based on the lattice Gross-Pitaevskii equation indicate that band structure renormalization is caused by the distortion of the overall lattice potential away from the kagome geometry by interactions.

DOI: 10.1103/PhysRevLett.125.133001

Band structure describes the states of motion of non-interacting particles within a spatially periodic potential, and helps explain properties of materials, the propagation of light in photonic crystals, and the transport of ultracold atoms within optical lattices. In some materials, interactions cause band structure to differ strongly from the noninteracting case, an effect known as band structure renormalization. Such renormalization can be particularly important in heavy-fermion materials, where the Fermi energy lies within a band with very small dispersion (a flat band) [1].

Flat bands have also been realized in optical lattices. Specifically, in the two-dimensional kagome [2] and Lieb [3] lattices, geometric frustration of particle motion produces nondispersing bands. In the tight-binding limit, with the tunneling energy between neighboring sites i and j defined as $-J(\hat{a}_i^\dagger \hat{a}_j + \hat{a}_j^\dagger \hat{a}_i)$, a flat band emerges as the third and second bands of the $J > 0$ kagome and Lieb lattices, respectively. Here, \hat{a}_i (\hat{a}_i^\dagger) is the particle annihilation (creation) operator at site i .

Systems of interacting bosons or fermions that equilibrate within flat bands are the subject of intense interest [4–12]. Specifically, for interacting bosons equilibrating in the flat ground band of a $J < 0$ kagome lattice, You *et al.* [5] propose that interactions renormalize the band structure, causing a stable superfluid to form at the K or Γ points of the Brillouin zone, where, self-consistently, the band energy is minimized.

Here, we probe the effects of interactions on the flat band of an optical kagome lattice with an atomic Bose gas. A Bose-Einstein condensate of ^{87}Rb atoms is prepared at rest,

accelerated, and then loaded adiabatically into an excited Bloch state of the ($J > 0$) kagome lattice with variable quasimomentum \mathbf{q} and band index n . We characterize this far-from-equilibrium state by measuring its momentum distribution and group velocity \mathbf{v}_g . We find the group velocity for atoms in the $n = 3$ band of the kagome lattice to be significantly larger than expected for noninteracting atoms. Through experiments and numerical calculations, we confirm that the unflattening of the band results from interaction-driven band structure renormalization. Our work verifies the physical picture suggested by Ref. [5] that a flat band is renormalized by mean-field interactions and becomes dispersive, and, more generally, demonstrates that the transport of lattice-trapped atoms can be significantly influenced by interactions. Recently, the distortion of the flat band of the Lieb lattice by an interacting gas in a superposition of band states has also been observed [13].

In the limit of vanishing potential depth, the band energy $E_n(\mathbf{q})$ in any lattice approaches the energy of a free particle with momentum $\mathbf{p} = \hbar\mathbf{k}$, and Bloch states $\Psi_{\mathbf{q}}^{(n)}(\mathbf{r})$ map onto plane waves $\Psi_{\mathbf{q}}^{(n)}(\mathbf{r}) \sim \exp(i\mathbf{k} \cdot \mathbf{r})$, where \mathbf{k} lies in the n th Brillouin zone and $\mathbf{k} = \mathbf{q}$ modulo reciprocal lattice vectors. This mapping provides a three-step protocol to transport all atoms within a Bose-Einstein condensate into any Bloch state of an optical lattice (Fig. 1). First, a condensate is formed at $\mathbf{k} = 0$ in the absence of an optical lattice. Second, the condensate is accelerated to a momentum $\hbar\mathbf{k}$ lying in the n th Brillouin zone. Third, the lattice potential is ramped on, mapping the condensate adiabatically into the $\mathbf{q} = \mathbf{k}$ Bloch state in the n th band [14,15].

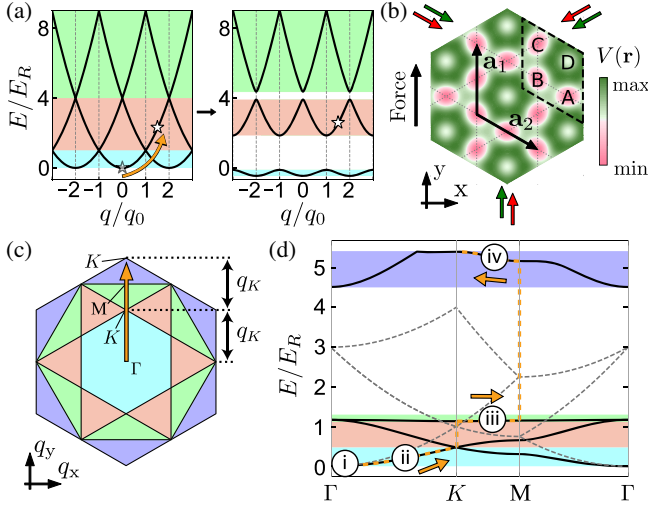


FIG. 1. Experimental scheme. (a) Illustration of the scheme with an example of one-dimensional system. The band structure of a 1D lattice, with lattice wave number $2 \times q_0$, at zero (left) and nonzero (right) depth in the extended zone scheme. A particle accelerated to the n th Brillouin zone ($n - 1 < |k|/q_0 < n$) is loaded adiabatically into the n th band as the lattice. (b) The optical kagome lattice is constructed by overlaying triangular lattices using short- (532 nm, green) and long-wavelength (1064 nm, shown in red) light. Primitive lattice vectors $\mathbf{a}_{1,2}$ are shown. The four sites in a unit cell are labeled A–D. (c) The first four Brillouin zones of the kagome lattice. Acceleration along \mathbf{y} maps atoms sequentially into the $n = 1$ (light blue, Γ to K), $n = 3$ (green, K to M), and then $n = 4$ (purple, M to K) bands. The orange trajectory indicates the range of wave vector \mathbf{k} atoms are accelerated to in experiments reported in Fig. 2. (d) Noninteracting band structure of the optical kagome lattice. Solid black lines: $(V_{SW}, V_{LW}) = \hbar \times (25, 15)$ kHz. Dashed gray lines: zero lattice depth. The yellow trajectory matches that in (c). Circled labels are referenced in Fig. 2(b). The recoil energy $E_R = \hbar \times 2.0$ kHz in the kagome lattice.

We prepare Bose-Einstein condensates of $0.4 - 22 \times 10^4$ ^{87}Rb atoms in an optical dipole trap with trap frequencies $\omega_{x,y,z} = 2\pi \times (23, 41, 46)$ Hz. A vertically (\mathbf{z}) oriented light beam at 1064 nm wavelength, with its focus displaced from the condensate in the x - y plane, is imposed for a variable time on the order of 1 ms. The dipole force of this beam accelerates the condensate at 6 m/s^2 in the \mathbf{y} direction. The $1/e^2$ radius of the beam ($85 \mu\text{m}$) is larger than the $R_{\text{TF}} \sim 10 \mu\text{m}$ Thomas-Fermi radii of the condensate, reducing effects of the imposed dipole potential curvature on the gas [16].

After the accelerating optical potential is switched off, we gradually impose an optical kagome lattice in the horizontal plane [2,17]. For this, we overlay two triangular lattices, created with short- (SW, 532 nm) and also long-wavelength (LW, 1064 nm) light with in-plane polarization. The depths of the two sublattices are increased to their final values in $T = 1.2$ ms [18]. The potential along the \mathbf{z} axis is unmodified by the lattice beams and remains loosely confining.

After allowing the gas to evolve within the lattice for $\leq 350 \mu\text{s}$, we characterize its momentum distribution. We suddenly switch off the optical lattice and dipole trap, allow the atoms to expand into a loosely confining magnetic trap for a quarter-cycle of harmonic oscillation, and then image them. This technique maps a Bloch state into a reciprocal lattice of sharply peaked atomic distributions.

Letting q_K be the magnitude of the quasimomentum at the first K point, accelerating atoms along \mathbf{y} to a wave vector \mathbf{k}/q_K in the ranges of (0,1), (1,1.5), and (1.5,2) places the gas into the first, third, and fourth bands of the lattice, respectively [Fig. 1(c)]. Since the condensate has negligible widths in momentum space approximated by $\hbar/R_{\text{TF}} = 0.02(0.01)\hbar q_K$ in the \mathbf{y} (\mathbf{x}) direction, the entire quantum gas can be loaded into a single band as long as one avoids the edges of the Brillouin zone, where our adiabatic-loading scheme fails.

Representative momentum distributions at four points along this trajectory are shown in Fig. 2(b). Qualitatively, these distributions match with those calculated for noninteracting atoms in our kagome lattice [Fig. 2(a)], indicating that, indeed, our procedure places the entire population of the condensate into excited Bloch states, including into the $n = 3$ band whose (noninteracting) band dispersion is near zero [19].

However, a quantitative analysis reveals dramatic differences from the noninteracting band model. We focus on the group velocity $\mathbf{v}_g = \hbar^{-1} \nabla_{\mathbf{q}} E_n(\mathbf{q})$. By the Hellmann-Feynman theorem [20–22], which applies regardless of interaction strength, the group velocity is related to the mean velocity $\mathbf{v}_g = \langle \hbar \mathbf{k} / m \rangle$ of the Bloch state, with m being the atomic mass.

Experimentally, we measure this mean velocity by applying spatial fits to the imaged distribution in a region surrounding each peak to determine the population $N_{\mathbf{G}}$ of atoms in the $\hbar(\mathbf{q} + \mathbf{G})$ momentum states, where \mathbf{G} are reciprocal lattice vectors. We then take the weighted average $\mathbf{v}_g = (\hbar/m) [\sum_{\mathbf{G}} (\mathbf{q} + \mathbf{G}) N_{\mathbf{G}}] / (\sum_{\mathbf{G}} N_{\mathbf{G}})$.

The observed group velocity disagrees profoundly with the noninteracting band structure result. In particular, whereas the noninteracting band theory predicts a near-zero group velocity within the $n = 3$ kagome-lattice band, we observe a gas of atoms loaded into that band to have a significantly higher group velocity.

To explain this disagreement, we consider effects of interactions. Band structure applies to interacting systems in various ways. One approach is to consider weak excitations atop an interacting equilibrium system characterized by lattice symmetry. The band excitation spectrum of interacting lattice-trapped quantum gases has been measured, e.g., by optical Bragg scattering [23–26].

Alternately, band structure may be used to describe the far from equilibrium state of a gas residing entirely in an excited Bloch state. For a condensed Bose gas, interactions are treated at the mean-field level by finding the Bloch states of the lattice Gross-Pitaevskii equation,

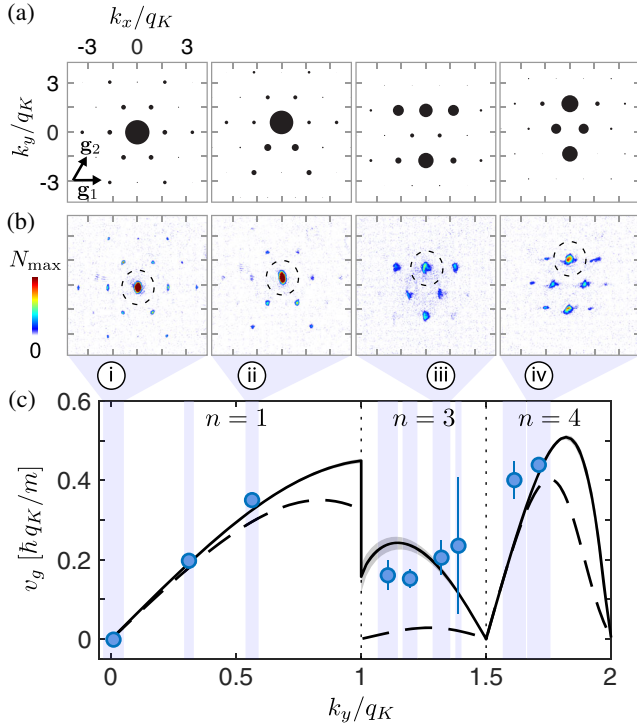


FIG. 2. Measured group velocity in the kagome lattice. Momentum distributions are shown [(a) noninteracting Bloch theory; (b) measured] at four representative initial \mathbf{k} [indicated by dashed circles in (b)] with labels corresponding to those in Fig. 1(d). Basis reciprocal lattice vectors $\mathbf{g}_{1,2}$ are shown. (c) Measured $v_g = \mathbf{v}_g \cdot \mathbf{y}$. The initial wave vector \mathbf{k} is measured for each experimental repetition. Data with k_y within a binning range (blue shaded bars) are averaged, with 3–8 measurements per bin. Error bars are standard mean errors. Data agree with calculations that include effects of interactions at a peak density of $n_0 = 5.4(5) \times 10^{13} \text{ cm}^{-3}$ (solid line, gray region indicates effect of density uncertainty), and disagree with noninteracting band-theory predictions (dashed line). Final lattice depths are $(V_{\text{SW}}, V_{\text{LW}}) = h \times (25, 15) \text{ kHz}$.

$$\left(-\frac{\hbar^2}{2m} \nabla^2 + V(\mathbf{r}) + g|\Psi(\mathbf{r})|^2 \right) \Psi(\mathbf{r}) = E_n(\mathbf{q})\Psi(\mathbf{r}) \quad (1)$$

where $g = 4\pi\hbar^2 a/m$ with a being the s -wave scattering length, and $\Psi(\mathbf{r})$ is the condensate wave function. Self-consistent Bloch-state solutions are found where the density $|\Psi(\mathbf{r})|^2$ is symmetric under translation by lattice vectors. The state $\Psi(\mathbf{r})$ is then a Bloch state for a noninteracting gas in an overall potential that is the sum of the applied lattice potential $V(\mathbf{r})$ and the spatially periodic interaction energy $g|\Psi(\mathbf{r})|^2$. Such solutions have been studied in the context of quantum gases, identifying additional solutions beyond those in the noninteracting case (swallowtails), related dynamical phenomena such as nonlinear Landau-Zener tunneling and hysteresis [27–36], and modulational instability [37–39]. Nonlinear Bloch modes also arise in nonlinear photonic crystals [40] and exciton-polariton condensates [41].

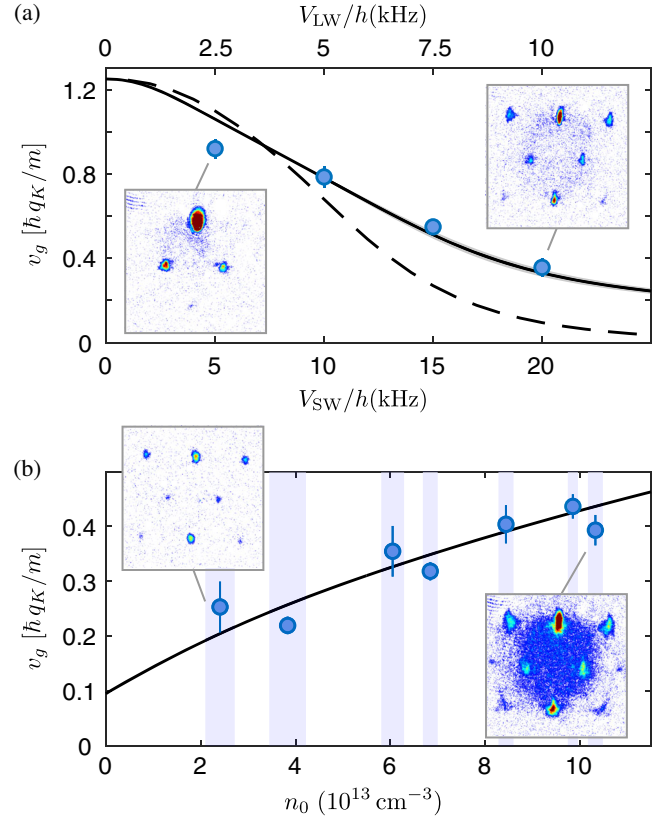


FIG. 3. Dependence of v_g on lattice depths and densities measured at a fixed initial wave vector of $k_y = 1.25q_K$. (a) v_g measured with a peak density $n_0 = 6.2(6) \times 10^{13} \text{ cm}^{-3}$ and different lattice depths ($V_{\text{SW}}/V_{\text{LW}}$ constant). While band theory (dashed line) predicts that v_g is suppressed quickly at increasing lattice depths, data (each point is average of 4–7 measurements) show a significantly smaller rate of suppression, in agreement with Gross-Pitaevskii equation predictions (solid line; gray region indicates effects of density uncertainty). (b) v_g measured at $(V_{\text{SW}}, V_{\text{LW}}) = h \times (20, 10) \text{ kHz}$ increases monotonically with number density as predicted by the Gross-Pitaevskii equation (black line). Data within a small binning range (blue shaded bars) of densities, determined up to 10% systematic uncertainty, are averaged, with 3–8 measurements per bin. Error bars are standard mean errors. Insets are single-shot images taken at indicated settings.

The group velocity determined from Eq. (1) agrees with our measurements [Fig. 2(c)] [42]. Both numerical and experimental data show that the effect of interactions on the group velocity is most pronounced in the $n = 3$ band.

We characterize the interaction-induced distortion of the kagome lattice flat band by two additional experiments. We focus on the initial wave vector $k_y = 1.25q_K$, within the $n = 3$ band. First, we measure v_g for identically prepared condensates that are loaded into lattices of increasing depth [Fig. 3(a)]. For the noninteracting case, the calculated group velocity tends quickly to zero as the lattice is deepened and approaches the kagome-geometry, tight-binding limit. In contrast, in the presence of interactions,

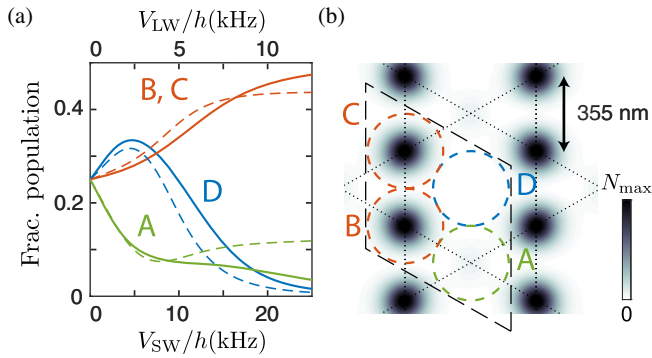


FIG. 4. Real-space distribution of atoms in the $n = 3$, $k_y = 1.25q_K$ Bloch state. (a) Calculated fractional population in the four kagome-lattice sites in a unit cell as a function of lattice depths with $V_{SW}/V_{LW} = 2$ (dashed line: band theory; solid line: Gross-Pitaevskii equation). (b) Real-space distribution of atoms in a lattice at $(V_{SW}, V_{LW}) = h \times (20, 10)$ kHz calculated by solving the Gross-Pitaevskii equation with $n_0 = 6.2 \times 10^{13} \text{ cm}^{-3}$.

while v_g diminishes for increasing lattice depth, it does so only slowly and lies significantly higher than the non-interacting result.

Second, we study the dependence of v_g on the interaction strength by varying the density of the gas. We load condensates with initial peak densities n_0 in the range of $2 - 11 \times 10^{13} \text{ cm}^{-3}$ into the aforementioned Bloch state, and find v_g increases with gas density [Fig. 3(b)], showing that the flat band of the kagome lattice acquires a dispersion that increases with interaction energy.

The picture that emerges from our findings is that the interaction among atoms within a Bloch state adds to and distorts the lattice potential, thereby changing the transport properties of the lattice. This distortion is evident in the real-space atomic distribution predicted by the lattice Gross-Pitaevskii equation. In Fig. 4, we consider again the $n = 3$, $k_y = 1.25q_K$ Bloch state, and calculate the population fractions in the four sites of the lattice unit cell, with A, B, and C being the three allowed sites in the kagome lattice, and D being the site excluded from the lattice as V_{LW} is increased. In the deep lattice, the population becomes concentrated largely in just two sites of the kagome lattice (B and C). The unequal population of atoms in the kagome lattice sites leads to a mean-field interaction potential that departs from the kagome-lattice geometry. The relevance of this potential can be quantified by the ratio of the characteristic interaction energy and the tunneling energy $n_0 g/J$, which is about 1 at the lattice depth and density considered here [43]. It is then not surprising that the band structure of this distorted overall lattice potential no longer supports a flat $n = 3$ band.

Our demonstrated ability to place a ^{87}Rb gas into the $n = 3$ band of a $J > 0$ kagome lattice raises the possibility that many-body states of interacting bosons in a flat band [4,5,12] may be studied through transient equilibration of atoms within an excited band. However, the excited-band

population in our experiment is unstable to decay, indicated by the sharp momentum peaks of the excited coherent Bloch state decaying to a broad momentum distribution [see, e.g., data for the highest-density gas in Fig. 3(b)]. This broad distribution grows to a significant fraction of the total atom population within hundreds of μs , with shorter lifetimes seen for higher-density gases in higher-depth lattices. Through band mapping, we determine that this decay produces atoms predominantly in the ground band. Examining also the evolution of atoms prepared in the $n = 2$ (reached by accelerating the gas initially along \mathbf{x}) or $n = 4$ bands, we observe the $n = 3$ Bloch state to decay most rapidly. It remains to be seen whether atoms prepared in energy extrema of the renormalized $n = 3$ band, predicted to lie at the Γ and K points, show greater stability. The decay to lower bands may occur through collisions that transfer energy into the loosely confined \mathbf{z} direction of motion. Such collisions may be forestalled by adding an additional confining lattice along \mathbf{z} .

In conclusion, in searching for experimental evidence of the nondispersing nature of the $n = 3$ band of the kagome lattice, we find, instead, that interactions among atoms placed within that band lead to significant band structure renormalization. The emergence of a modified overall lattice structure generated by atoms within a lattice is reminiscent of experiments on quantum gases within optical cavities [44,45]. In the optical-cavity experiments, the emergent lattice is generated by light-induced extended-range atomic interactions, whereas, in the present work, the emergent potential is produced by direct local interactions. Future work may examine which aspects of the noninteracting band structure become invalid for lattice-trapped interacting systems, e.g., by studying the interplay between hysteresis and band-geometry effects.

We thank Storm Weiner and Leon Lu for experimental assistance and valuable discussions. This work was supported by the NSF, and by the AFOSR and ARO through the MURI program (Grants No. FA9550-14-1-0035 and No. W911NF-17-1-0323, respectively). G. U. acknowledges support by the Austrian Science Fund FWF within the DK-ALM (Grant No. W1259-N27).

- [1] G. Zwicknagl, *Adv. Phys.* **41**, 203 (1992).
- [2] G.-B. Jo, J. Guzman, C.K. Thomas, P. Hosur, A. Vishwanath, and D.M. Stamper-Kurn, *Phys. Rev. Lett.* **108**, 045305 (2012).
- [3] S. Taie, H. Ozawa, T. Ichinose, T. Nishio, S. Nakajima, and Y. Takahashi, *Sci. Adv.* **1**, e1500854 (2015).
- [4] S.D. Huber and E. Altman, *Phys. Rev. B* **82**, 184502 (2010).
- [5] Y.-Z. You, Z. Chen, X.-Q. Sun, and H. Zhai, *Phys. Rev. Lett.* **109**, 265302 (2012).
- [6] S. Maiti and T. Sedrakyan, *Phys. Rev. B* **99**, 174418 (2019).

- [7] H.-Y. Hui, Y. Zhang, C. Zhang, and V. W. Scarola, *Phys. Rev. A* **95**, 033603 (2017).
- [8] M. Tovmasyan, E. P. L. van Nieuwenburg, and S. D. Huber, *Phys. Rev. B* **88**, 220510(R) (2013).
- [9] H. Tasaki, *Phys. Rev. Lett.* **69**, 1608 (1992).
- [10] M. Imada and M. Kohno, *Phys. Rev. Lett.* **84**, 143 (2000).
- [11] V. I. Iglovikov, F. Hébert, B. Grémaud, G. G. Batrouni, and R. T. Scalettar, *Phys. Rev. B* **90**, 094506 (2014).
- [12] S. A. Parameswaran, I. Kimchi, A. M. Turner, D. M. Stamper-Kurn, and A. Vishwanath, *Phys. Rev. Lett.* **110**, 125301 (2013).
- [13] H. Ozawa, S. Taie, T. Ichinose, and Y. Takahashi, *Phys. Rev. Lett.* **118**, 175301 (2017).
- [14] L. Fallani, F. S. Cataliotti, J. Catani, C. Fort, M. Modugno, M. Zawada, and M. Inguscio, *Phys. Rev. Lett.* **91**, 240405 (2003).
- [15] A. Browaeys, H. Häffner, C. McKenzie, S. L. Rolston, K. Helmerson, and W. D. Phillips, *Phys. Rev. A* **72**, 053605 (2005).
- [16] Residual curvature effects increase the peak density n_0 by $\sim 15\%$.
- [17] C. K. Thomas, T. H. Barter, T.-H. Leung, M. Okano, G.-B. Jo, J. Guzman, I. Kimchi, A. Vishwanath, and D. M. Stamper-Kurn, *Phys. Rev. Lett.* **119**, 100402 (2017).
- [18] The SW (LW) lattices are ramped up from initial values $V_i = h \times 0.5$ (0.4) kHz to their final values $V_f = V_{\text{SW}}$ (V_{LW}) as $V(t) = V_i + (V_f - V_i)(e^{\alpha t/T} - 1)/(e^\alpha - 1)$, where $\alpha = 2.5$ and $T = 1.2$ ms. The initial values, required for stabilization, do not affect the accelerating condensate. Ramp parameters are chosen based on simulations that indicate a minimum state fidelity of 99%, 95%, and 90% for the $n = 1$, $n = 3$, and $n = 4$ bands, respectively.
- [19] For faster ramp-up, we observe temporal oscillations in the momentum-space populations at the final lattice depths, indicating that the atoms occupy a superposition of multiple bands and that the state fidelity is lowered. In contrast, for the $T = 1.2$ ms ramp-time data, we observe no such oscillations.
- [20] P. Güttinger, *Z. Phys.* **73**, 169 (1932).
- [21] H. Hellmann, *Z. Phys.* **85**, 180 (1933).
- [22] R. P. Feynman, *Phys. Rev.* **56**, 340 (1939).
- [23] D. Clément, N. Fabbri, L. Fallani, C. Fort, and M. Inguscio, *Phys. Rev. Lett.* **102**, 155301 (2009).
- [24] X. Du, S. P. Wan, E. Yesilada, C. Ryu, D. J. Heinzen, Z. X. Liang, and B. A. Wu, *New J. Phys.* **12**, 083025 (2010).
- [25] P. T. Ernst, S. Gotze, J. S. Krauser, K. Pyka, D.-S. Luhmann, D. Pfannkuche, and K. Sengstock, *Nat. Phys.* **6**, 56 (2010).
- [26] X. Liu, X. Zhou, W. Zhang, T. Vogt, B. Lu, X. Yue, and X. Chen, *Phys. Rev. A* **83**, 063604 (2011).
- [27] B. Wu and Q. Niu, *Phys. Rev. A* **61**, 023402 (2000).
- [28] J. Liu, L. Fu, B.-Y. Ou, S.-G. Chen, D.-I. Choi, B. Wu, and Q. Niu, *Phys. Rev. A* **66**, 023404 (2002).
- [29] B. Wu, R. B. Diener, and Q. Niu, *Phys. Rev. A* **65**, 025601 (2002).
- [30] D. Diakonov, L. M. Jensen, C. J. Pethick, and H. Smith, *Phys. Rev. A* **66**, 013604 (2002).
- [31] E. J. Mueller, *Phys. Rev. A* **66**, 063603 (2002).
- [32] M. Machholm, C. J. Pethick, and H. Smith, *Phys. Rev. A* **67**, 053613 (2003).
- [33] B. T. Seaman, L. D. Carr, and M. J. Holland, *Phys. Rev. A* **71**, 033622 (2005).
- [34] Z. Chen and B. Wu, *Phys. Rev. Lett.* **107**, 065301 (2011).
- [35] S. B. Koller, E. A. Goldschmidt, R. C. Brown, R. Wyllie, R. M. Wilson, and J. V. Porto, *Phys. Rev. A* **94**, 063634 (2016).
- [36] M. Machholm, A. Nicolin, C. J. Pethick, and H. Smith, *Phys. Rev. A* **69**, 043604 (2004).
- [37] B. Wu and Q. Niu, *Phys. Rev. A* **64**, 061603(R) (2001).
- [38] V. V. Konotop and M. Salerno, *Phys. Rev. A* **65**, 021602(R) (2002).
- [39] L. Fallani, L. De Sarlo, J. E. Lye, M. Modugno, R. Saers, C. Fort, and M. Inguscio, *Phys. Rev. Lett.* **93**, 140406 (2004).
- [40] D. Träger, R. Fischer, D. N. Neshev, A. A. Sukhorukov, C. Denz, W. Królikowski, and Y. S. Kivshar, *Opt. Express* **14**, 1913 (2006).
- [41] I. Y. Chestnov, A. V. Yulin, A. P. Alodjants, and O. A. Egorov, *Phys. Rev. B* **94**, 094306 (2016).
- [42] For this calculation, we identify those solutions of Eq. (1) that map smoothly those of the noninteracting system with the corresponding band index.
- [43] R. Walters, G. Cotugno, T. H. Johnson, S. R. Clark, and D. Jaksch, *Phys. Rev. A* **87**, 043613 (2013).
- [44] S. Gopalakrishnan, B. L. Lev, and P. M. Goldbart, *Nat. Phys.* **5**, 845 (2009).
- [45] R. Mottl, F. Brennecke, K. Baumann, R. Landig, T. Donner, and T. Esslinger, *Science* **336**, 1570 (2012).

Correction: An affiliation was inadvertently duplicated that rearranged the numbering during the production process. The affiliation list has been fixed.